Available online at www.sciencedirect.com

ScienceDirect

Physics Letters B 641 (2006) 486–490

PHYSICS LETTERS B

www.elsevier.com/locate/physletb

Addendum

Addendum to: "Threshold corrections to m_b and the $\bar{b}b \to H_i^0$ production in CP-violating SUSY scenarios" [Phys. Lett. B 595 (2004) 347]

Francesca Borzumati [a,b,*], Jae Sik Lee [c]

[a] *International Center for Theoretical Physics, Trieste, Italy*
[b] *Scuola Internazionale Superiore di Studi Avanzati, Trieste, Italy*
[c] *Centre for Theoretical Physics, Seoul National University, Seoul, Republic of Korea*

Received 26 July 2006; accepted 19 August 2006

Available online 31 August 2006

Editor: T. Yanagida

The production cross sections of the three neutral Higgs bosons through b-quark fusion can deviate substantially from those obtained in CP-conserving scenarios, thanks to the nontrivial role that the threshold corrections to m_b can play in them [1]. The largest deviations in the case of H_1 and H_2 are for values of $\Phi_{A\mu}$ around 100°, with a large enhancement for the production cross section of H_1, a large suppression for that of H_2. The former is due to the fact that the component of the field a in H_1 around these values of $\Phi_{A\mu}$ is large, while it is depleted by a similarly large amount in H_2. The cross section for H_3 is also largely affected by the m_b corrections, but this deviation is roughly independent of $\Phi_{A\mu}$.

In this region of large mixings the H_1 and H_2 bosons have very similar masses, as shown in the first column of Fig. 1, where the masses are plotted versus $\Phi_{A\mu}$ for three different values of $\Phi_{g\mu}$: 0°, 90°, 180°. In the first and third column of this figure, the solid lines always represent H_1, the dashed lines H_2, the long-dashed ones H_3. When mixings are maximal, the H_1–H_2 mass difference is always below 5 GeV, as shown by the second column of the same figure and the width of H_1 is always about 10 times larger than that of H_2, see third column. Likewise, the production cross section of H_1 is also always one order of magnitude larger than that of H_2, both at the LHC and at the Tevatron.

Given the degeneracy between H_1 and H_2, it is legitimate to worry whether a transition $H_1 \to H_2$ can occur during propagation and before decay, due to the off-diagonal absorbtive parts in the 3×3 matrix for the propagator of the neutral Higgs bosons considered in Ref. [2]. We have numerically checked the size of these off-diagonal parts and found that in our specific case they are negligible. We have nevertheless included these terms in our numerical calculations. Thus, near $\sqrt{\hat{s}} = m_{H_i}$, the partonic cross section for the $\bar{b}b$-fusion production of H_i and their subsequent decay into a final state f.s., $\hat{\sigma}(\bar{b}b \to H_i \to \text{f.s.})$, hereafter denoted as $\hat{\sigma}^{\text{f.s.}}$, is given, to a very good approximation, by the cross section with a single $\hat{s}$-channel resonance with mass m_{H_i} and width Γ_{H_i}. Away from $\sqrt{\hat{s}} = m_{H_i}$, all Higgs bosons H_i contribute to the partonic cross section for the production of the same final state f.s.

The mass difference between H_1 and H_2 is, however, still small enough to question whether it is possible to disentangle the two corresponding peaks in the invariant mass distributions of the H_1- and H_2-decay products. There is no similar problem for the H_3 eigenstate, that has a mass always larger than ~ 160 GeV and therefore a splitting from H_2 always larger than ~ 10 GeV. Since $\Gamma_{H_2,H_3} \lesssim 2$–3 GeV, we assume that this splitting can be experimentally resolved. As already observed, on the contrary, in the case of H_1 and H_2, the mass difference can be as small 2 GeV around $\Phi_A = 100°$. It will therefore be very challenging to disentangle H_2 from H_1 experimentally. An analysis of the decay modes of these two Higgs bosons, of their differential cross section with respect to the invariant mass distribution of the decay products, and the experimental resolution of these decays, can help in this sense.

DOI of original article: 10.1016/j.physletb.2004.06.040.

* Corresponding author.
E-mail address: francesca.borzumati@cern.ch (F. Borzumati).

doi:10.1016/j.physletb.2006.08.042

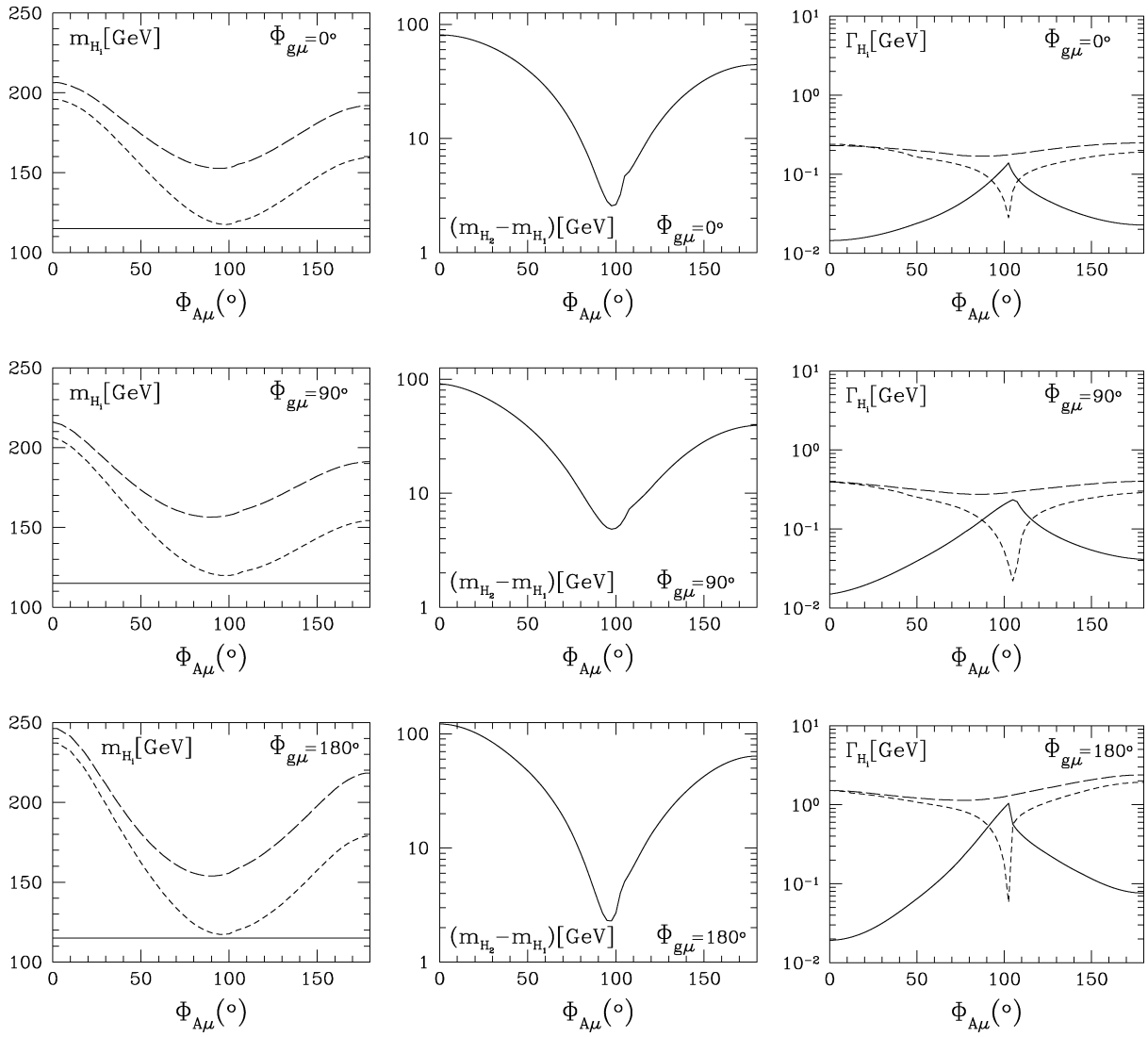

Fig. 1. The masses (left column) and widths (right column) of the neutral Higgs bosons as functions of $\Phi_{A\mu}$ for the CPX spectrum specified in Ref. [1] with $M_{\rm SUSY} = 0.5$ TeV and $\tan\beta = 10$. Three values of $\Phi_{g\mu}$ are considered: 0° (top row), 90° (middle row) and 180° (bottom row). The solid lines are for H_1, the dashed ones for H_2, and the long-dashed ones for H_3. The central column shows the mass difference between H_2 and H_1.

For our discussion we shall concentrate on the issue of production and possible problem of detection of H_1 and H_2 at the LHC only, where the best energy and momentum resolutions are for the Higgs-boson decays into muon and photon pairs. For these two decay modes, the invariant-mass resolutions are, respectively, $\delta M_{\gamma\gamma} \sim 1$ GeV and $\delta M_{\mu\mu} \sim 3$ GeV for a Higgs mass of ~ 100 GeV [3].

The H_i-differential production cross section through b-quark fusion with respect to the invariant mass distribution of the final state f.s. ($=\gamma\gamma$ or $\bar\mu\mu$) is

$$\frac{\mathrm{d}\sigma^{\rm f.s.}}{\mathrm{d}\sqrt{\hat s}} = \frac{2}{\sqrt{\hat s}}\hat\sigma^{\rm f.s.}(\tau)\left(\tau\frac{\mathrm{d}\mathcal{L}^{\bar bb}}{\mathrm{d}\tau}\right) = \frac{2}{\sqrt{\hat s}}\hat\sigma^{\rm f.s.}(\tau)\int_\tau^1 \mathrm{d}x\left[\frac{\tau}{x}b_{\rm had_1}(x,Q)\bar b_{\rm had_2}\left(\frac{\tau}{x},Q\right) + (b\leftrightarrow\bar b)\right], \tag{1}$$

where $\tau \equiv \hat s/s$, with s the centre-of-mass energy squared of the considered hadron collider. The symbols $b_{\rm had_i}(x,Q)$ and $\bar b_{\rm had_i}(x,Q)$ indicate the b- and $\bar b$-quark distribution functions in the hadron had$_i$, and had$_1$ had$_2$ are pp at the LHC (they would be $p\bar p$ at the Tevatron). The partonic cross section $\hat\sigma^{\rm f.s.}(\hat s)$ can be written in a compact way for both final states $\bar\mu\mu$ and $\gamma\gamma$ as follows:

$$\hat\sigma^{\rm f.s.}(\hat s) = \frac{g_b^2 g_{\rm f.s.}^2}{16\pi\hat s}\frac{\beta_{\rm f.s.}}{\beta_b}\frac{1}{4}\frac{1}{3}\frac{1}{N_{\rm f.s.}}\sum_{\sigma,\lambda}\left|\langle\lambda;\sigma\rangle^{\rm f.s.}\right|^2, \tag{2}$$

where $\beta_f = (1 - 4m_f^2/\hat{s})^{1/2}$, $g_f = gm_f/2M_W = m_f/v$, and

$$g_{\text{f.s.}} = \begin{cases} \alpha\sqrt{\hat{s}}/4\pi v, \\ g_\mu, \end{cases} \qquad \beta_{\text{f.s.}} = \begin{cases} 1, \\ \beta_\mu, \end{cases} \qquad N_{\text{f.s.}} = \begin{cases} 2, \\ 1, \end{cases} \quad \text{for f.s.} = \begin{cases} \gamma\gamma, \\ \bar{\mu}\mu. \end{cases} \tag{3}$$

Finally, $\langle\lambda;\sigma\rangle^{\text{f.s.}}$ is the reduced helicity amplitude for the process $\bar{b}b \to H_i \to$ f.s. and $\sum_{\sigma,\lambda}$ indicate the sum over the helicities of the initial b-quarks, σ, and of the outgoing γ's or μ's, λ. For f.s. $= \gamma\gamma$ it is:

$$\langle\lambda;\sigma\rangle^{\gamma\gamma} \equiv \sum_{i,j} \left(\sigma\beta_b g^S_{H_i\bar{b}b} + ig^P_{H_i\bar{b}b}\right) D_{ij}(\hat{s}) \left[S^\gamma_j(\hat{s}) - i\lambda P^\gamma_j(\hat{s})\right], \tag{4}$$

for f.s. $= \bar{\mu}\mu$:

$$\langle\lambda;\sigma\rangle^{\mu\mu} \equiv \sum_{i,j} \left(\sigma\beta_b g^S_{H_i\bar{b}b} + ig^P_{H_i\bar{b}b}\right) D_{ij}(\hat{s}) \left(\lambda\beta_\mu g^S_{H_j\bar{\mu}\mu} - ig^P_{H_j\bar{\mu}\mu}\right). \tag{5}$$

In both, D_{ij} is the 3×3 propagator matrix, which, as already mentioned, has negligible off-diagonal terms in the specific case under consideration; $g^{S,P}_{H_i\bar{b}b}$ are the couplings denoted as $g^{S,P}_{H_i}$ in Eqs. (15) and (16) of Ref. [1], and the symbols $g^{S,P}_{H_j\bar{\mu}\mu}$ are: $g^S_{H_j\bar{\mu}\mu} = O_{\phi_1 j}/\cos\beta$ and $g^P_{H_j\bar{\mu}\mu} = -O_{aj}\tan\beta$. The effective neutral Higgs boson couplings to two photons $S^\gamma_j(\hat{s})$ and $P^\gamma_j(\hat{s})$ can be found in Ref. [4].

As previously stated, in our specific case, near $\sqrt{\hat{s}} = m_{H_i}$, the cross section $\hat{\sigma}^{\text{f.s.}}$ is well approximated by the cross section with a single $\hat{s}$-channel resonance with mass m_{H_i} and width Γ_{H_i}. The form of the helicity amplitudes in Eqs. (4) and (5) can be simplified in such a way that $\hat{\sigma}^{\text{f.s.}}$ and $\mathrm{d}\sigma^{\text{f.s.}}/\mathrm{d}\sqrt{\hat{s}}$ reduce to the simple forms:

$$\hat{\sigma}^{\text{f.s.}}(\hat{s}) \underset{\hat{s}\to m^2_{H_i}}{\approx} \frac{1}{\pi} \frac{\sigma(\bar{b}b \to H_i)}{\Gamma_{H_i}} \text{BR}(H_i \to \text{f.s.}) m_{H_i}, \tag{6}$$

$$\frac{\mathrm{d}\sigma^{\text{f.s.}}}{\mathrm{d}\sqrt{\hat{s}}} \underset{\hat{s}\to m^2_{H_i}}{\approx} \frac{2}{\pi} \frac{\sigma(\bar{b}b \to H_i)}{\Gamma_{H_i}} \text{BR}(H_i \to \text{f.s.}) \left(\tau \frac{\mathrm{d}\mathcal{L}^{\bar{b}b}}{\mathrm{d}\tau}\right), \tag{7}$$

where $\sigma(\bar{b}b \to H_i)$ is the partonic cross section for the production of H_i through b-quark fusion, shown in Ref. [1]. The dominant contribution to the widths Γ_{H_1} and Γ_{H_2} comes from the decays $H_{1,2} \to \bar{b}b$, at $\Phi_{A\mu} \sim 100^\circ$. In this region, therefore, the ratios $\sigma(\bar{b}b \to H_i)/\Gamma_{H_i}$ are roughly independent of $\Phi_{A\mu}$, whereas $\sigma(\bar{b}b \to H_i)$ and Γ_{H_i}, separately, are strongly dependent on it. Thus, still for $\Phi_{A\mu} \sim 100^\circ$, given the degeneracy of H_1 and H_2, the relative heights of the peaks of $\hat{\sigma}^{\text{f.s.}}$ and $\mathrm{d}\sigma^{\text{f.s.}}/\mathrm{d}\sqrt{\hat{s}}$ at $\hat{s} = m^2_{H_1}$ and $\hat{s} = m^2_{H_2}$ are practically determined by BR($H_i \to$ f.s.) only.

In Figs. 2 and 3, we compare the values of both, the partonic cross section $\hat{\sigma}^{\text{f.s.}}$ and the differential hadronic cross section $\mathrm{d}\sigma^{\text{f.s.}}/\mathrm{d}\sqrt{\hat{s}}$ for f.s. $= \gamma\gamma$ and f.s. $= \bar{\mu}\mu$ at two different values of $\Phi_{A\mu}$: 100° and 105°. These two values of $\Phi_{A\mu}$ are sufficiently close to avoid a substantial reduction of the enhancing factor for $\sigma(\bar{b}b \to H_1)$ when going from $\Phi_{A\mu} = 100^\circ$ to $\Phi_{A\mu} = 105^\circ$. They are, however, separated enough for us to escape at $\Phi_{A\mu} = 105^\circ$ the strong suppression that $\sigma(\bar{b}b \to H_2)$ and Γ_{H_2} have at $\Phi_{A\mu} = 100^\circ$.

For an easier comparison of the cross sections obtained for the two different decay channels of H_1 and H_2, we list explicitly in Table 1 the values of m_{H_i}, Γ_{H_i}, $\sigma(\bar{b}b \to H_i)$, BR($H_i \to \gamma\gamma$), and BR($H_i \to \bar{\mu}\mu$) at $\Phi_{A\mu} = 100^\circ$ and 105°. We notice:

- Going from $\Phi_{A\mu} = 100^\circ$ to $\Phi_{A\mu} = 105^\circ$, the mass of H_2 increases by less than 2.5 GeV. It is, at these two values of $\Phi_{A\mu}$, respectively only about 3 and 5 GeV larger than m_{H_1}, which, as explained in Ref. [1], has been fixed to 115 GeV for all values of $\Phi_{A\mu}$.
- At $\Phi_{A\mu} = 100^\circ$, as already observed in Ref. [1], the value of the partonic cross sections $\sigma(\bar{b}b \to H_1)$ is about five times larger than $\sigma(\bar{b}b \to H_2)$. Similarly, Γ_{H_2} is suppressed with respect to Γ_{H_1} also by a factor of five. At $\Phi_{A\mu} = 105^\circ$, on the contrary, both cross sections and widths for H_1 and H_2 are remarkably similar, and only a factor of 1.5–2 less than the maximal values of $\sigma(\bar{b}b \to H_1)$ and Γ_{H_1} obtained at $\Phi_{A\mu} = 100^\circ$.
- As for the branching ratios of H_1 and H_2 into $\gamma\gamma$ and $\bar{\mu}\mu$, we notice that at $\Phi_{A\mu} = 100^\circ$, the branching ratio BR($H_1 \to \gamma\gamma$) is about two order of magnitude smaller than BR($H_2 \to \gamma\gamma$), whereas it is of the same order of (actually 50% larger than) BR($H_2 \to \gamma\gamma$) at $\Phi_{A\mu} = 105^\circ$. The strong suppression of BR($H_1 \to \gamma\gamma$) at $\Phi_{A\mu} = 100^\circ$ is due to the large component of a in H_1 at this value of $\Phi_{A\mu}$. On the contrary, the branching ratios BR($H_1 \to \mu\mu$) and BR($H_2 \to \mu\mu$) are of the same size for both values of $\Phi_{A\mu}$ considered.

Therefore, at $\Phi_{A\mu} = 100^\circ$, when the neutral Higgs bosons decay into a pair of photons, we expect to see only one peak corresponding to H_2. Given the values of the invariant mass distribution in the lower-left frame of Fig. 2, for a luminosity of 100 fb^{-1}, we expect to have ~ 50 events in the $\sqrt{\hat{s}}$ interval $[m_{H_2} - \delta M_{\gamma\gamma}/2, m_{H_2} + \delta M_{\gamma\gamma}/2]$, with $\delta M_{\gamma\gamma}$ the experimental invariant mass

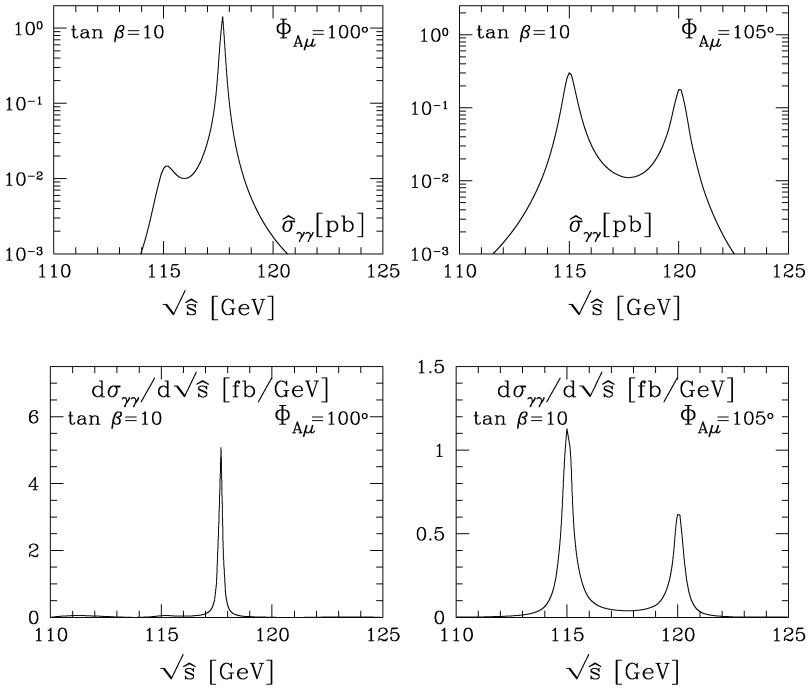

Fig. 2. Cross sections $\hat{\sigma}^{\gamma\gamma}$ (upper two frames) and $\mathrm{d}\sigma^{\gamma\gamma}/\mathrm{d}\sqrt{\hat{s}}$ (lower two frames) at $\Phi_{A\mu} = 100^\circ$ and $\Phi_{A\mu} = 105^\circ$, versus $\sqrt{\hat{s}}$. In all frames, it is $\tan\beta = 10$ and $\Phi_{g\mu} = 180^\circ$.

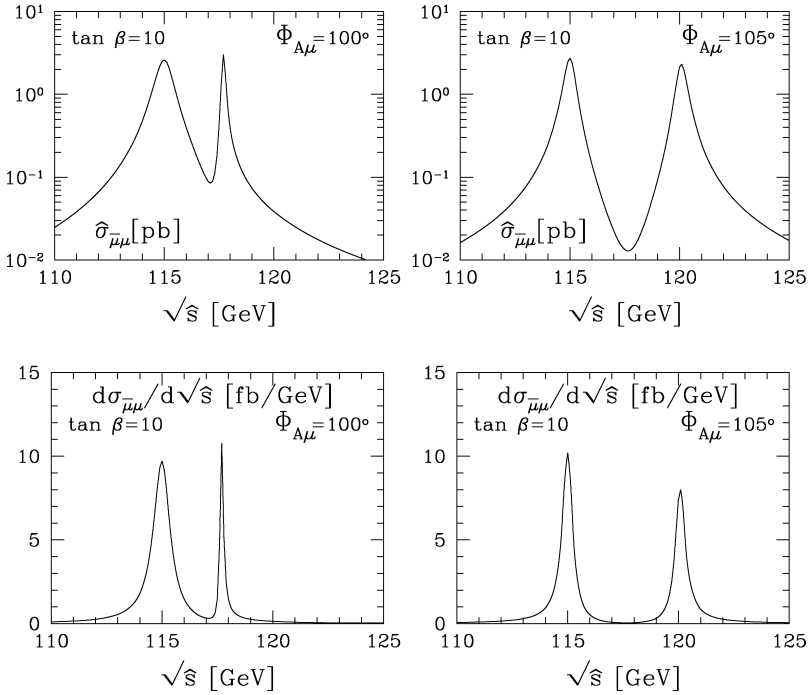

Fig. 3. Same as in Fig. 2 for $\hat{\sigma}^{\bar{\mu}\mu}$ (upper two frames) and $\mathrm{d}\sigma^{\bar{\mu}\mu}/\mathrm{d}\sqrt{\hat{s}}$ (lower two frames).

resolution mentioned above, ~ 1 GeV. When $\Phi_{A\mu} = 105^\circ$, it is possible to detect two peaks and have, for the same luminosity, more than 30 (20) events in the two $\sqrt{\hat{s}}$ intervals of 1 GeV centered around m_{H_1} and m_{H_2}.

When H_1 and H_2 decay into a muon pair, although the cross sections are larger, a resolution of the two picks will be more difficult because of the worse experimental resolution $\delta M_{\mu\mu} \sim 3$ GeV. At $\Phi_{A\mu} = 100^\circ$, again for a luminosity of 100 fb^{-1}, it is possible to have more than 1,000 events in the interval $[m_{H_1} - \delta M_{\mu\mu}/2, m_{H_1} + \delta M_{\mu\mu}/2]$, and 200 events in $[m_{H_2} - \delta M_{\mu\mu}/2, m_{H_2} + \delta M_{\mu\mu}/2]$. Notice that H_2 is only 2.7 GeV away from H_1. For $\Phi_{A\mu} = 105^\circ$, more than 300 events are expected for both peaks, separated by 5 GeV, see the lower-right frame of Fig. 3.

Table 1
For H_1 and H_2 at two different values of $\Phi_{A\mu}$, 100°, 105°, we list here the values of: masses and widths (in GeV), partonic cross sections for their resonant production (in pb) and branching ratios of their decays into a pair of μ's and a pair of γ's. $\Phi_{g\mu}$ is fixed at 180° and $\tan\beta$ at 10

	$\Phi_{A\mu}$	m_{H_i} [GeV]	Γ_{H_i} [GeV]	$\sigma(\bar{b}b \to H_i)$ [pb]	BR($H_i \to \bar{\mu}\mu$)	BR($H_i \to \gamma\gamma$)
H_1	100°	115.0	0.9157	786.7	8.227×10^{-5}	3.996×10^{-7}
H_1	105°	115.0	0.5664	486.3	8.654×10^{-5}	9.883×10^{-6}
H_2	100°	117.7	0.1818	145.3	9.978×10^{-5}	4.858×10^{-5}
H_2	105°	120.1	0.5652	429.4	7.953×10^{-5}	6.219×10^{-6}

For both values of $\Phi_{A\mu}$, by combining the muon-decay mode with the photon-decay mode, H_2 can be located more precisely and disentangled from H_1. At $\Phi_{A\mu} = 105°$, actually, two well separated peaks may be observed. It is clear that these considerations are only a first step towards more dedicated analyses, which obviously require detector simulations and background studies.

Acknowledgements

The authors thank G. Polesello for discussions. The work of J.S.L. was supported in part by the Korea Research Foundation and the Korean Federation of Science and Technology Societies Grant funded by the Korean Government (MOEHRD, Basic Research Promotion Fund).

References

[1] F. Borzumati, J.S. Lee, W.Y. Song, Phys. Lett. B 595 (2004) 347, hep-ph/0401024.
[2] J.R. Ellis, J.S. Lee, A. Pilaftsis, Phys. Rev. D 70 (2004) 075010, hep-ph/0404167.
[3] Atlas Collaboration, Atlas: detector and physics performance technical design report, vol. 2, CERN-LHCC-99-15, ATLAS-TDR-15, 1999.
[4] J.S. Lee, A. Pilaftsis, M. Carena, S.Y. Choi, M. Drees, J.R. Ellis, C.E.M. Wagner, Comput. Phys. Commun. 156 (2004) 283, hep-ph/0307377.